International Journal of Current Engineering and Technology
E-ISSN 2277 – 4106, P-ISSN 2347 – 5161
©2022 INPRESSCO®, All Rights Reserved
Available at http://inpressco.com/category/ijcet

Research Article

Numerical Analysis of Vertical Pile Subjected to an Inclined Eccentric Load

Fathi M. Abdrabbo†, Khaled E. Gaaver ‡ and Musab M. Eldooma†

†,‡Structural engineering department, Faculty of Engineering, Alexandria University, Egypt.
†Civil engineering department, Faculty of Engineering science, University of Nyala, Sudan.

Received 18 July 2022, Accepted 10 Aug 2022, Available online 15 Aug 2022, **Vol.12, No.4 (July/Aug 2022)**

Abstract

Contradictory behavior of vertical pile subjected to inclined load was found in literature, so the current research was devoted to investigates the behavior of single vertical steel hollow pipe pile embedded in sand subjected to compressive inclined eccentric load through MIDAS GTS/NX 2019 FEM package. 3D numerical analysis simulating the pile-soil system have been carried out. The effects of the loading inclination angle and the pile length and diameter on the performance of the pile were investigated. Inclined load carrying capacity and pile stiffness as well as lateral deformation profiles along the pile were presented. The pile head displacement and pile stiffness are significantly affected by loading inclination angle. It was observed that, P-Y curves of the pile-soil system are independent of loading inclination angle α. also the pile length and diameter are markedly affecting the behavior of the pile.

Keywords: *Deep foundation, Inclined load, Piles, Pile deformations.*

1. Introduction

Many structures supported on piles are subjected to inclined compressive loads (R) such as electrical transmission towers, wind energy converter towers, and offshore structures. Due to the complex cases of the applied loading conditions on such structures, the supporting pile foundation should satisfy the safety and serviceability requirement as well. Most often the axial loads on piles supporting a structure are predominant. But in special cases like piles supporting offshore wind energy converter towers, the vertical load is minor compared by lateral load as pointed out by Zang et al. [1]. The study of vertical pile subjected to inclined loading (R) was investigated during 70s of the last century on the basis of experimental results from loading tests performed on small-scale piles, Meyerhof and his co-researches[2–4]. While theoretical analyses for assessing the ultimate bearing capacity (R_u) of a vertical pile subjected to an inclined load were proposed by Meyerhof and Ranjan [5].

In case of inclined loaded pile, current design practice involves independent analysis of vertical and lateral pile capacities and does not consider the interactions of vertical and horizontal load components (R_v and R_h).

*Corresponding authors ORCID ID: 0000-0000-0000-0000
DOI: https://doi.org/10.14741/ijcet/v.12.4.8

Therefore, to predict the load-displacement response of a vertical pile under inclined load, it is assumed that the lateral displacement (U_h) of the pile head is independent of the vertical component of the inclined load (R_v). Similarly, while estimating the ultimate lateral resistance (R_{uh}), it is considered that the vertical load component (R_v) of the inclined load does not influence the ultimate lateral resistance of the pile (R_{uh}) [6]. However, Analytical investigations carried out by Davisson and Robinson [7], Ramasamy, [8], and Goryunov [9] revealed that, the lateral deflection of a pile due lateral load increases with the combination of vertical loads. But experimental investigation carried out by Pise [10], Sarochan and Bykov [11] and Jain et al. [12], as well as field investigations conducted by Bartolomey [13] and Zhukov and Balov [14], revealed that a decrease in lateral deflection with the combination of vertical load. Anagnostopoulos, and Georgiadis [15] attributed this contrary in pile response under inclined load to the procedure adopted for pile-soil modelling.

Flexible reinforced concrete piles subjected to inclined load at the pile head can experience a flexural or an axial response depending upon load inclination angle (α), conte et al. [16]. Also, the bearing capacity of a pile (R_u)under inclined load is highly dependent on the load inclination angle (α) and the structural properties of the pile material [16]. The combined loading (R_v) and (R_h) Significantly increases the lateral

capacity (R_{uh}) of a vertical pile in sandy soil, Karthigeyan et al. [17]. Karthigeyan attributed this increase to the increase of vertical stress at pile-soil interface due to vertical load compared to the case of no vertical load on the pile head.

Hu et al., 2022 studied numerically the effect of the soil layering on the response of a laterally loaded monopile in sandy soil and predicted an empirical equations to calculate the load-displacement response of the pile [18].

The paper presents 3D numerical analysis of inclined loaded vertical pile in loose sand, where the objectives were; (1) study the effect of pre-vertical load (R_v) acting on the pile head on the performance of laterally loaded pile, and the effect of pre-lateral load (R_h) acting on the pile head on the performance of vertically loaded pile. (2) Investigating the effect of load inclination angle (α) on the inclination angle (β) of pile head displacement vector (U). (3) investigating the effect of load inclination angle (α) on the ultimate inclined load (R_u), and on serviceability load (R_s). and (4) study the effects of load inclination angle (α) on p-y relationship. (5) studying the effect of load eccentricity (e) on the performance of the pile.

2. Model configuration and mesh discretization

An extensive 3-D numerical investigation using finite element software MIDAS GTS/NX, 2019 has been performed. The study aimed to a better understanding of the behaviour of vertical pile under the effect of an inclined load (R).

Steel pipe piles of different embedded lengths (L) and different diameters (D) with wall thickness (t) of 50.0 mm embedded in loose sand have been analyzed. The pile was modelled as linear, elastic, and non-porous material with a unit weight of γ = 78 KN/m3, modulus of elasticity E = 210 GPa, and Poisson's ratio ν=0.2. While the soil has been modelled as loose sand simulated under undrained condition by using Modified Mohr-Coulomb constitutive model (MMC) built in software, table (1).

A typical mesh discretization used in the study is shown in the Fig. (1). The boundaries of the model were simulated using the automatic constraint built in the software in which the vertical boundary was constraint against any lateral movement, only vertical movement was allowed. The bottom boundary was constrained against the movement in all directions.

The vertical boundaries were located at a distance(X) equal to 32 times the pile diameter from center of the pile. While the bottom boundary was located at a distance (Y) equal to about 16 times the pile diameter measured from the ground surface which is corresponding to 2.6L as illustrated in Fig. (1). The pile was assumed to be filed with sand of the same properties as the outside sand up to ground surface, internal friction along the pile were considered.

The mesh around the pile was refined to avoid stress concentration zones effects. The interface between the pile and the soil, outside and inside, was modelled using the strength reduction factor built in software. The recommended value of Strength Reduction Factor SRF was 0.6.

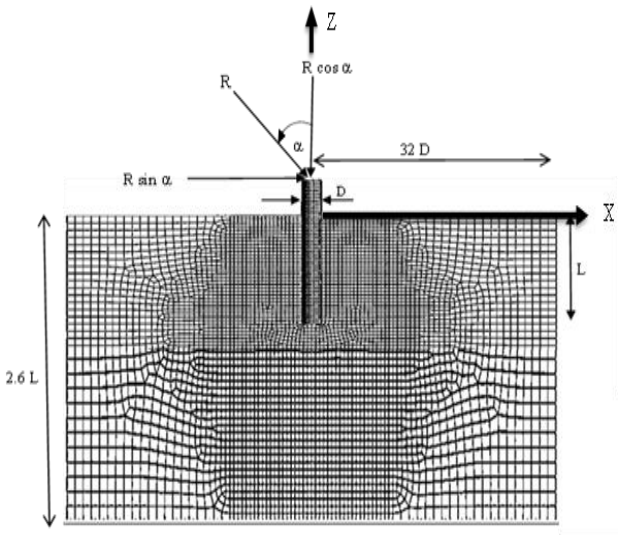

Fig. 1. Model Mesh and sign conventions

3. Simulation Process

The initial step was to simulate the soil body force using K_0-state, K_0 was taken as equal to (1- sinΦ). Followed by construction stage that the steel pile was activated as well as the interface between the pile and the soil, then the displacements which were resulted from these two steps were cleared to zero. In loading stage, each inclination loading angle (α) has a corresponding loading situation consists of a couple of lateral and vertical load components (R_h and R_v) which are applied simultaneously to provide a resultant load (R) with a constant inclination angle (α) with vertical.

Each loading consists of 100 incremental loading steps for each α. The load components R_h and R_v were adopted to generate different inclination angle (α) of the resultant load (R) by using load control condition.

Another type of loading conditions were applied. In these conditions, the vertical load (V) was applied incrementally up to a certain percentage of the ultimate vertical load (V_u) of the pile, and kept constant, then the lateral load (H) was applied incrementally up to a lateral displacement equal to 10% of the pile diameter. Also, the pile was loaded incrementally to a certain percentage of ultimate lateral load (H_u) and kept constant then the vertical load was applied incrementally up to a vertical displacement equal to 10% of the pile diameter.

Table 1 Undrained soil parameter after [12]

Parameter	Value	unit
Unit weight (ɤ)	16.5	KN/m3
Young's modulus (E_{oed}^{ref}) (Tangential Stiffness in oedometer test loading)	25000	KN/m2
Secant stiffness in standard drained triaxial test (E_{50}^{ref})	25000	KN/m2
Elastic modulus at unloading (E_{ur}^{ref})	75000	KN/m2
Poisson's ratio (μ)	0.3	-
Undrained Cohesion (Cu)	0.1	KN/m2
Friction angle (ϕ)	27	[°]
dilatancy angle (ψ)	0	[°]
Lateral earth pressure coefficient (K0)	0.54	-

4. Model Validation

To ensure reasonable precision of the developed numerical model, the obtained results were compared by field, laboratory and numerical results documented in the literature [13], [14] on laterally loaded pile since the behavior of vertical pile due to inclined load is scarce in literature especially experimental results from full-scale pile load tests. Results from two different sources were implemented in validation.

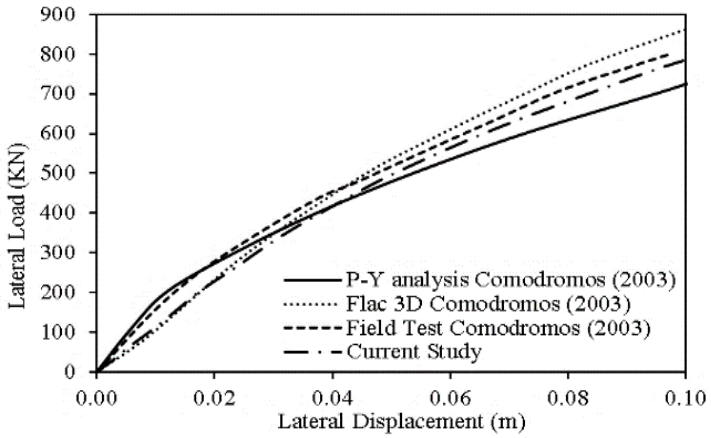

Fig. 2 Validation of the current model with Comodromos [13].

Fig. (2). revealed that the p-y method overestimates the lateral displacement of the pile at high load by up to 30%, while the numerical analysis carried by Comodromos [13] using FLAC 3D software underestimate the lateral displacement by up to 16%. While the current results agree reasonably with the full-scale test result.

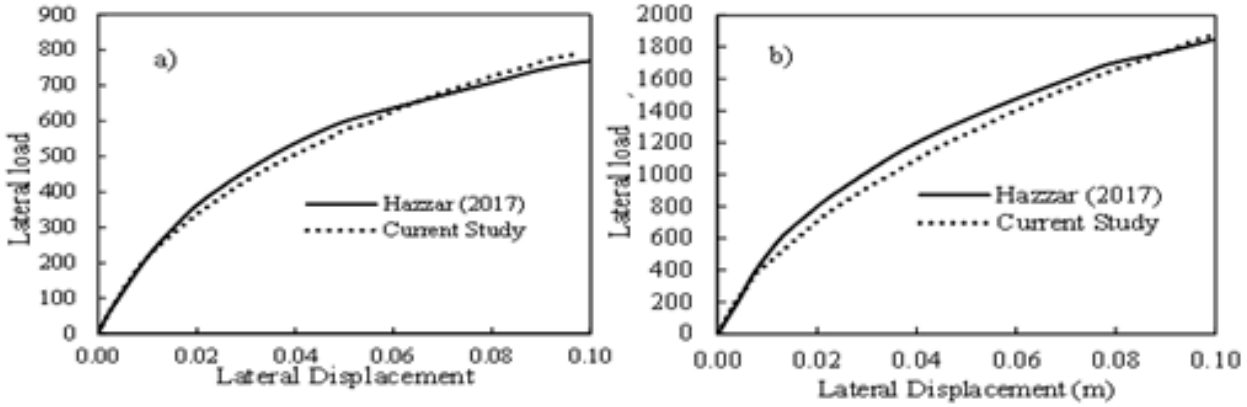

Fig. 3 Validation of the current model with Hazzar et al. [14], a) Very loose sand and b) Dense sand.

B. Validation (2)

Table 2 Properties of soil after [13]

Thickness of the layer (m)	Material type	Constitute model	Density (KN/m^3)	Elastic modulus (E) (MPa)	Poisson ratio (ν)	Friction angle (deg)	Dilation angle (deg)	Cohesion (kPa)
0-36	Soft clay	Mohr Coulomb	20	2.7	0.45	0	0	27
36-48	Medium-stiff clay	Mohr Coulomb	20	11.0	0.45	0	0	110
48-70	V. Dense sand	Mohr Coulomb	22	100.0	0.3	40	10	0
0-52	pile	Elastic	25	25000	0.2	--	--	--

Table 3 Properties of soil stated by [14]

Material type	Constitutive model	Mass density (KN/m^3)	Shear modulus G (MPa)	Bulk modulus K (MPa)	Angle of friction (°)	Interface coefficient μ
Very loose sand	Mohr Coulomb	1600	4.6	10.0	26	0.326
Loose to medium sand	Mohr Coulomb	1800	7.7	16.7	30	0.386
Dense sand	Mohr Coulomb	2000	19.2	41.7	36	0.486
Pile	Elastic	2500	10.4	13.9	--	

Table 4 Equivalent constitutive mode used in current study

Material type	Mass density (KN/m^3)	Elastic modulus E (MPa)	Poisson ratio ν	Angle of friction (°)
Very loose sand	16	12.0	0.3	26
Loose to Medium sand	18	20.0	0.3	30
Dense sand	20	49.9	0.3	36
Pile	25	25000	0.2	--

A. Validation (1)

The field load test conducted by Comodromos [13] was simulated using MIDAS GTS/NX 2019. The field tests were conducted on a large diameter concrete pile of 1.0 m diameter and 52 m length embedded in stratified soil layers shown in Table (2). Ground water table was located at the ground surface. The pile was simulated as elastic material, its properties shown in Table (2). While the interface between the pile and the soil was simulated using the strength reduction factor (SRF) of 0.6 as recommended by the software for steel-soil contact. The vretical boundary was taken at 32 times the pile diameter from pile center line. Whereas the bottom boundary was set at the bottom of the last soil layer depth 70.0 m from the ground surface. A lateral load increments were applied to the pile head until the lateral displacement attended 10% of the pile diameter at which the maximum load capacity of the pile was considered.

Second validation was conducted by comparing the results of the current study with that obtained by Hazzar et al. [14]. The authors simulated concrete pile of 1.0 m diameter and length of 10.0 m embedded in sand of different state conditions. Soil constitutive model and pile properties are presented in table (3). The vertical boundary used in the analysis was located at depth equal to 32 times the pile diameter from the center line of the pile and the bottom boundary was located at a distance equal to 1.6 times the pile length (L) from the ground surface. The pile was loaded laterally at the pile head up to a lateral displacement equal to 10% of the pile diameter using displacement control approach. The authors used FLAC 3D software in their analysis. The constitutive model of the pile and the soil implemented in FLAC 3D were developed in terms of bulk modulus (K) and shear Modulus (G) of sand which are not suitable input soil parameters to be used in Midas GTS/NX software.

Therefore, the elastic modulus (E) and Poisson's ratio (ν) needed in MIDAS software were calculated using G and K via Equation (1) and Equation (2), table (4).

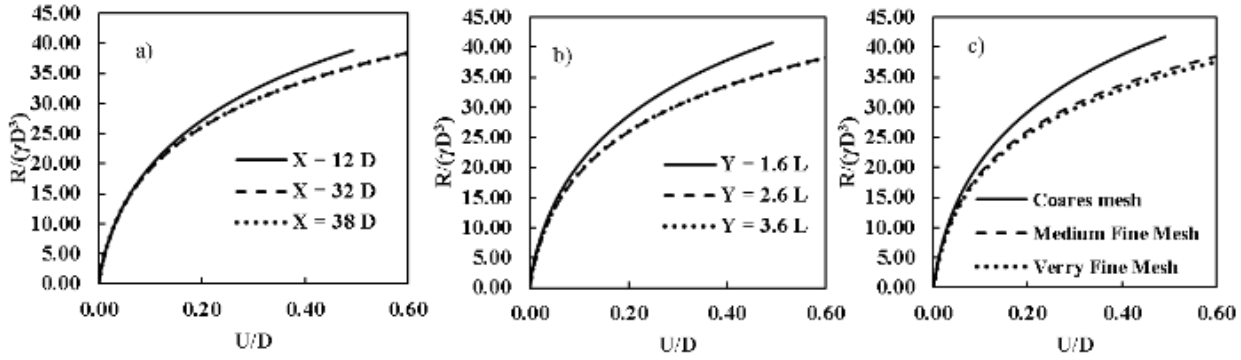

Fig. 4 Sensitivity analysis of the model; a) horizontal boundary, b) vertical boundary and c) mesh fineness

$$E = \frac{9KG}{3K+G} \quad (1)$$

$$\nu = \frac{3K-2G}{2(3K+G)} \quad (2)$$

The lateral displacement-load relationship at the pile head obtained from the current study compared well with that obtained by Hazzar et al. [14]. Fig. (3).

5. Sensitivity analysis

Preliminary analyses of the mesh fineness and the geometry of the soil domain were carried out to assess the configuration of finite element mesh and size of soil domain in order to reduce computational effort without sacrificing accuracy.

The effect of the location of lateral boundary from the pile center line (X) and the depth of the soil domain (Y) as well as the mesh fineness around the pile on the response of a pile loaded at 45˚ is shown in Fig (4). The figure revealed that a domain of size (X=32D), (Y=2.6L) provided with medium fine mesh are suitable to avoid boundary effects and save computation time.

6. Parametric Study

An extensive 3D numerical analysis simulating the pile soil system have been made using MIDAS GTS/NX, 2019 Package. The piles are extending above ground surface a distance (e) and embedded in sandy soil to a depth (L). The pile is subjected to inclined load (R) at the pile head.

The spatial parameters implemented in the parametric study are, the pile geometry (L and D), the loading inclination angle α, and the load eccentricity (e).

7. Results and discussion

7.1. The Pre-load effect:

Fig. (5) presents the response of the pile due to lateral load when pre-vertical load (v) was applied first. The pre-vertical load was applied incrementally to a specific load level (V/Vu) and kept constant then a lateral load (H) was applied incrementally up to a lateral displacement of the pile head equal to 0.1 D was achieved. Different values of pre-vertical load levels (V/V_u) were applied.

Fig (5) revealed that there are no appreciable effects of the pre-vertical load on the lateral displacement of the pile due to lateral load. And consequently, the lateral load capacity of the pile may be estimated irrespective of the effect of vertical load. The figure indicates that the lateral stiffness of the pile is not affected by the vertical load. These results are in contradictory with Kartigejan [17], but agree with that reported by Abdel-Rahman et al[19].

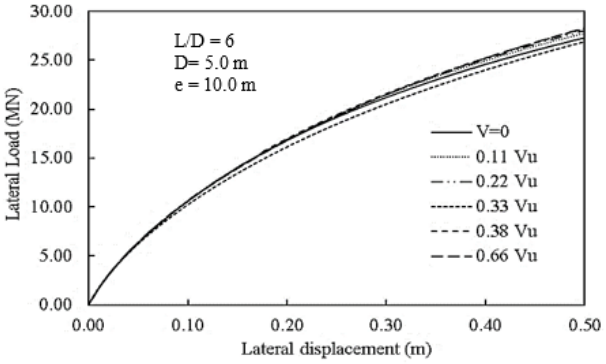

Fig. 5 The effect of the pre-vertical load on the horizontal behavior of the pile

Fig. (6) presents the effect of pre-lateral load (H/H_u) on the vertical response of the pile due to vertical load. The vertical loads were applied incrementally whereas the lateral load was kept constant at a specific load level (H/H_u). The figures revealed that at small pre-lateral load level (H/H_u) less than 15%, there is no appreciable effect of pre-lateral load on the axial response of the pile due to vertical load. But at higher lateral load level (H/H_u), the pre-lateral loads were markedly affected the vertical response of the pile. The ultimate vertical capacity of the pile increases with the increase of the lateral load level. Therefore, the ultimate lateral capacity of the pile as well as the lateral stiffness of the pile-soil system may be estimated irrespective of pile vertical load, but the ultimate vertical load depends upon the pre-lateral load bigger than 15%H_u.

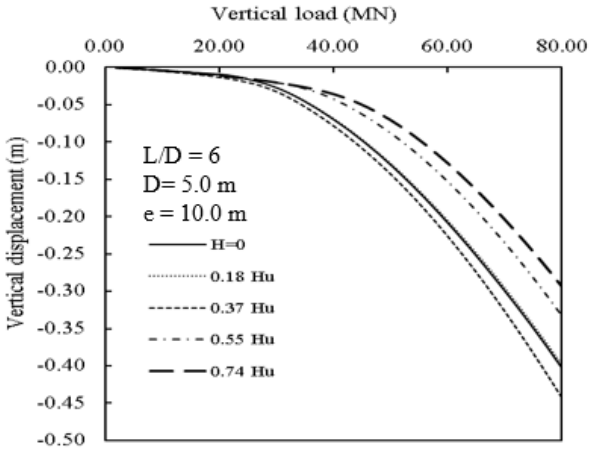

Fig. 6 The effect of the pre-lateral load on the vertical behavior of the pile

7.2. Pile Load-Displacement relationship under inclined load

An inclined load (R) acting on the pile produces horizontal displacement (Uh) and vertical displacement (Uv) of the pile head and rotation (θ). The resultant displacement is (U). the ultimate load Ru of the pile was assessed at displacement (U) equal to 0.1D while the serviceability load at pile head rotation equal to 0.25˚. Fig. (7), indicates that the initial stiffness of the pile (Kg) and the ultimate load (Ru), increased with the decrease of the inclination load angle (α). This is attributed to the increase of vertical component (Rv) of the inclined load. The results agree with Conte et al. 2015 [16]. Fig. (7) and (8) revealed that for α equal to 15˚ and more, the displacement vector (U) is resulted mainly from horizontal displacement component (Uh).

Comparison of Fig. (8) with Fig. (9) revealed that, the lateral displacement is the control of the ultimate load (Ru) of the pile, since a lateral displacement component (Uh) of 10% (D) is achieved at smaller load R compared by that load producing the same vertical displacement. Therefore, for α equal to and bigger than 15˚, the pile exhibits flexural behavior, and a passive wedge is developing in the soil along the top portion of the pile with shear displacement of soil oblique upward. For values of α less than 15˚, the axial behavior of the pile is prevailing, with the downward shear displacement of soil along the full length of the pile, and at the pile tip.

Fig. (8) through (10) reveal that with the increase of load inclination angle (α), the vertical displacement component (Uv) decreased while, the lateral displacement component (Uh) increased, and the rotation of the pile head increased.

The displacement vector (U) has an inclination angle (β) with the vertical bigger than the load inclination angle (α). The angle β varies from zero when the load R acting in vertical direction to π/2, when the load R acting in the lateral direction, Fig (11). The figure shows that, at serviceability load (Rs) and ultimate load (Ru), the inclination angle of the displacement vector (β) increased with the decrease of the pile length (L), since (Uh) increases, as long as α less than 45˚. Beyond this limit of α there is no appreciable effect of load inclination angle (α) on the displacement inclination angle β, since β approaching π/2. But it is worth noting that there is no appreciable effect of pile length (L) on the inclination angle (β) of the pile head displacement vector (U).

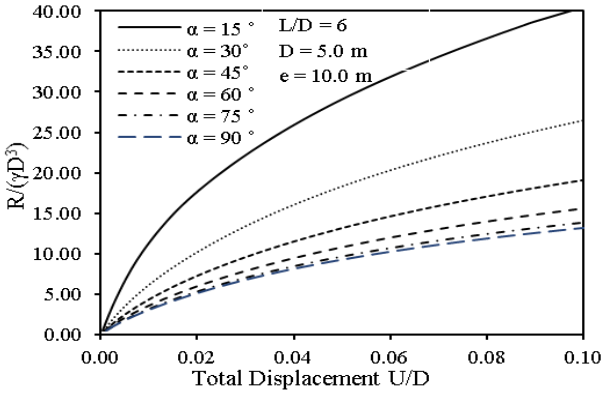

Fig. 7 Total displacement-load curve for different values of α.

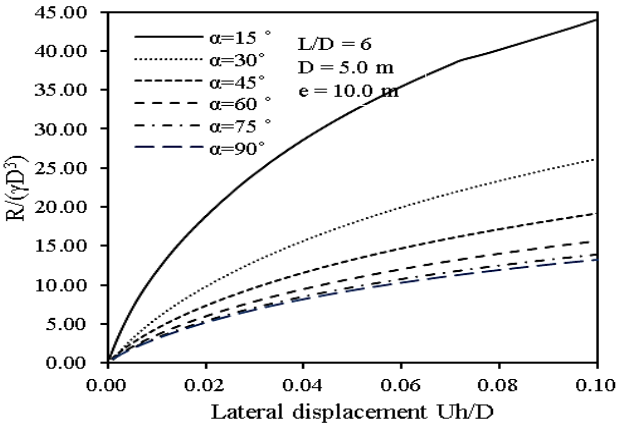

Fig. 8 Lateral displacement-load curve for different values of α.

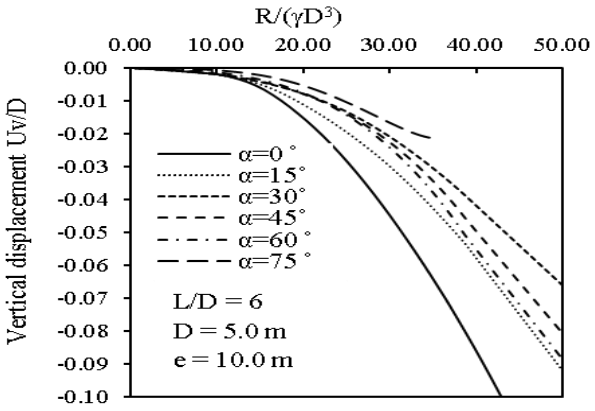

Fig. 9 Vertical displacement-load curve for different values of α.

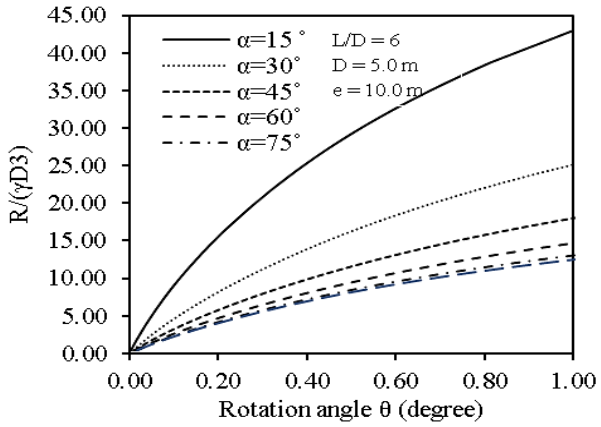

Fig. 10 Pile head rotation angle-load relationship for different values of α.

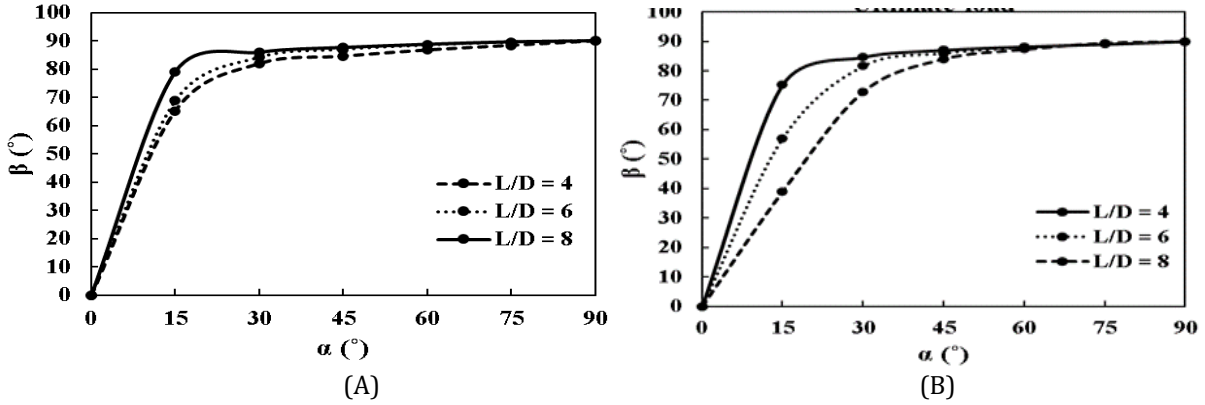

Fig. 11 The inclination angle (β) of displacement vector (U) for varies load angle (α), a) at serviceability load, b) at ultimate load

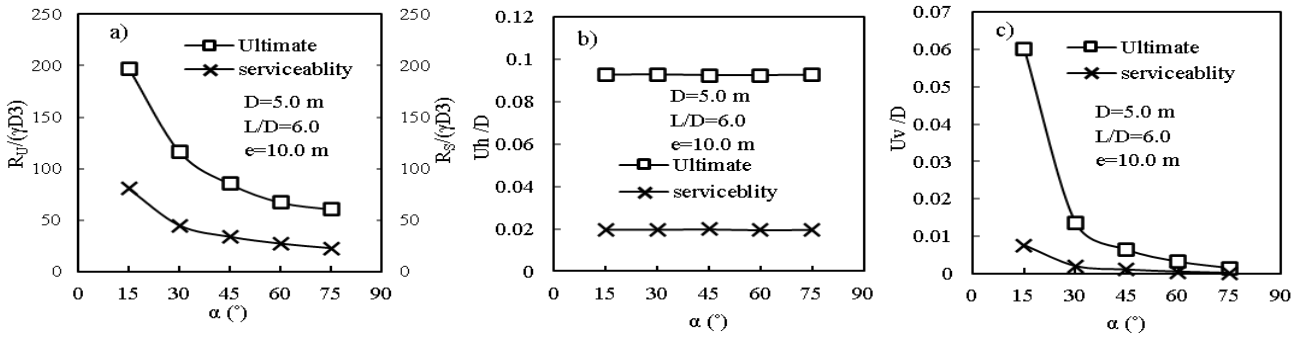

Fig. 12: a) Ultimate and serviceability loads due to rotation limit. B) horizontal displacement corresponding to ultimate and serviceability loads. c) vertical displacement corresponding to ultimate and serviceability loads

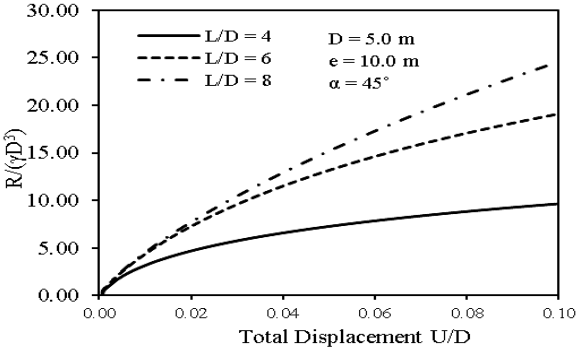

Fig. 13 Total displacement-load curve for different values of α and different values of pile lengths.

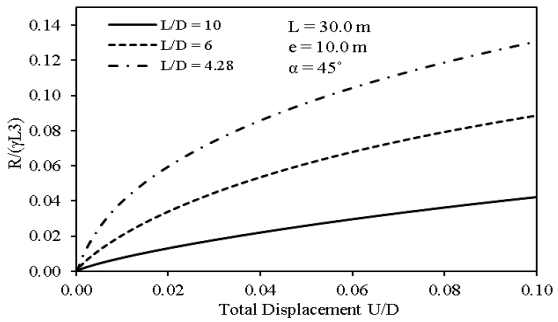

Fig. 14 Total displacement-load curve for different values of pile diameters.

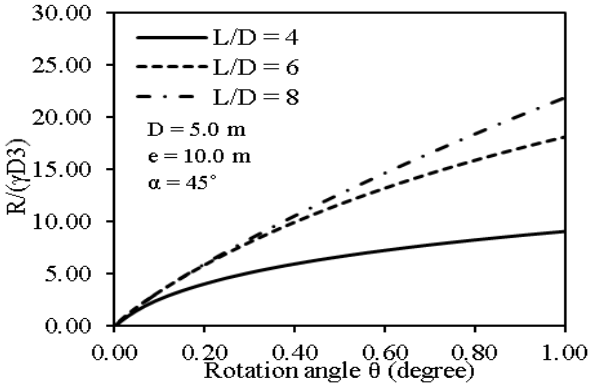

Fig. 15 Pile head rotation angle-load relationship for different values of pile lengths.

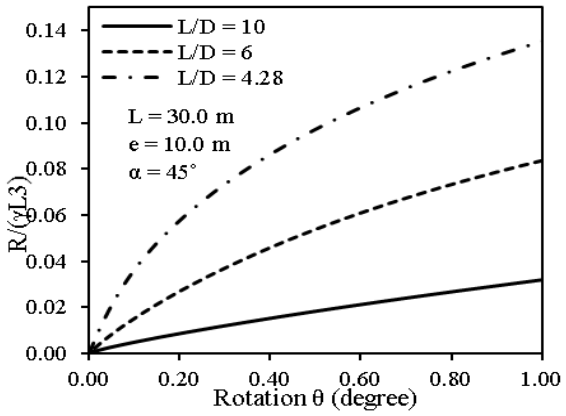

Fig. 16 Pile head rotation angle-load relationship for different values of pile diameters.

7.3 Ultimate and serviceability inclined load

Fig. (12) indicates that the ultimate load (Ru) and the serviceability load (Rs) are highly dependent on the load inclination angle (α). The serviceability load (Rs) produces vertical displacement of pile head less than 1.0% of pile diameter. Fig. (12-c) but with horizontal displacement (Uh/D) of about 2% D. The ultimate load (Ru) produces horizontal displacement of about 9% D and vertical displacement decreasing with α from 6% D to value less than %5 D at α less than 45°.

7.4 Effect of pile geometry (L and D)

Fig. (13) indicates that the pile ultimate load (Ru) increases with the increase of the pile embedment length (L) as well as the initial tangent stiffness, but it seems that the effect of pile length more than 30 m in the initial tangent stiffness is not pronounced.

The increase of pile ultimate load is attributed to the increase of the mobilized friction stresses along the pile shaft and the increase of bearing stresses at the pile base. For long piles the pile vertical stiffness is mainly due to friction developed along the pile shaft and little contributed by bearing stress at pile base. Therefore, the increase of the pile length from 30.0 m to 40.0 m contribute very little on pile vertical stiffness (Kv). At the mean time the increase of pile length beyond the pile critical length (Lc) has not appreciably affected pile lateral stiffness, (Kh).

Fig. (14) presents the effect of the pile diameter (D) on the response of the pile of length 30 m. The initial tangent stiffness and the pile ultimate load increased with the increase of pile diameter (D).

Fig. (15) and Fig. (16) show the effect of pile length (L) and pile diameter (D) on pile head rotation (θ) of a pile loaded by inclined load at α equal to 45°. The lateral displacement of the pile decreases with the increase of pile diameter and with the increase of pile length, due to the increase of pile lateral stiffness, therefore the pile head rotation decreased as well. At small inclined load, (R/γD3) less than 10, the rotation of the pile is not critically affected by the pile length bigger than 30 m. The results supported that the pile critical length (Lc) is not only the soil-pile parameters but also depends on pile head load level.

Fig. (17) and Fig. (18) present a polar diagram of the ultimate loads (Ru). The ultimate loads were presented as a polar for each inclination angle (α). Whereas the y-coordinate representing the vertical components (Ruv) of the ultimate load (Ru) while, x-coordinate representing the lateral components (Ruh).

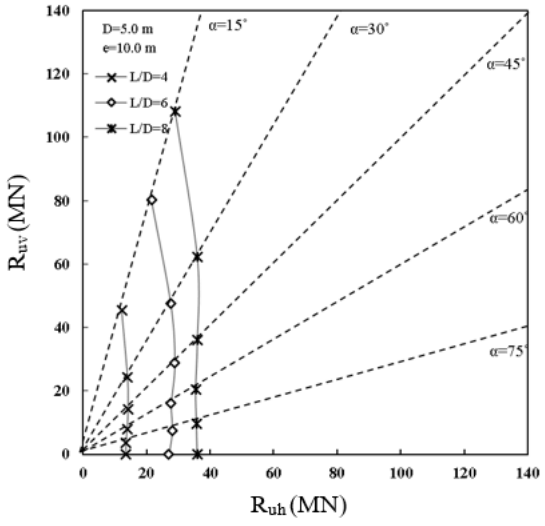

Fig. 17 Ultimate load at polar diagram and its component for various pile lengths

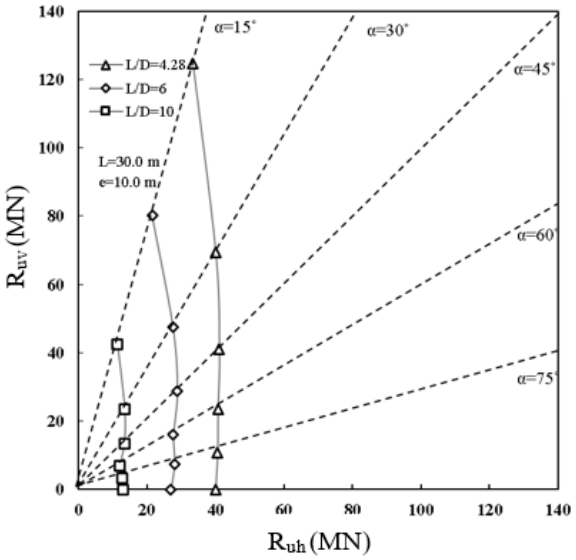

Fig. 18 Ultimate load at polar diagram and its component for various pile lengths

The figures revealed that the ultimate loads (Ru) and the corresponding vertical components (Ruv) are decreasing with the increase of load inclination angle (α). While the horizontal components (Ruh) are independent of α except at α equal to 15°. The horizontal component of the ultimate load (Ru) increases with the increase of pile diameter and pile length as well as the vertical components.

7.5 p-y relationship

The following is an attempt to explore the effect of load inclination angle (α) on p-y curves of piles embedded in loose sand. The p-y curves at different pile depths resulted from inclined load R acting at various inclination angles (α) are presented in Fig. 19. Where p is the horizontal stress at certain pile depth (z) (KN/m) and y is the corresponding horizontal displacement normalized as (y/D).

The figure revealed that the p-y relationships are independent of α.

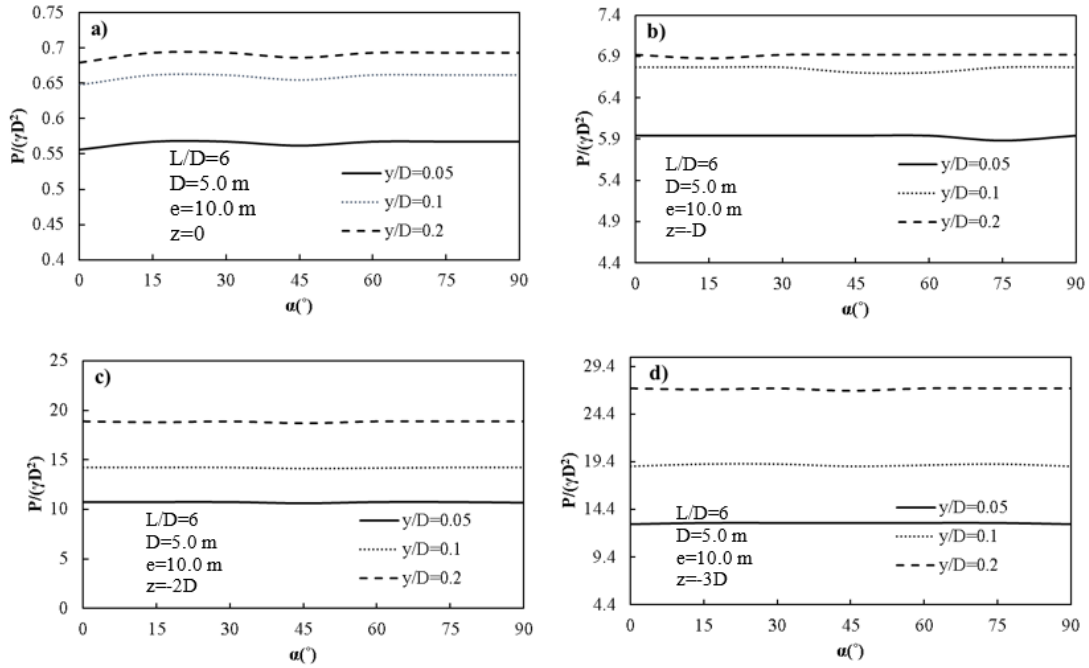

Fig. 19 p-y relationships along the pile at various inclination angle (α).

7.6 Effect of load eccentricity (e)

Fig. 20 presents the effect of load eccentric (e) on the ultimate load of the pile for various values of load eccentricity (e). The figure reveals that the load eccentricity (e) has an appreciable effect on the ultimate load of the inclined loaded piles. However, the effect is negligible when α is equal to zero. Note that when α equals zero, there is no effect of the eccentricity (e) on the ultimate load due to the absence of the horizontal component of the inclined load (R), which results in the additional bending moment to the pile. The ultimate inclined load increases with the decrease of load eccentricity (e).

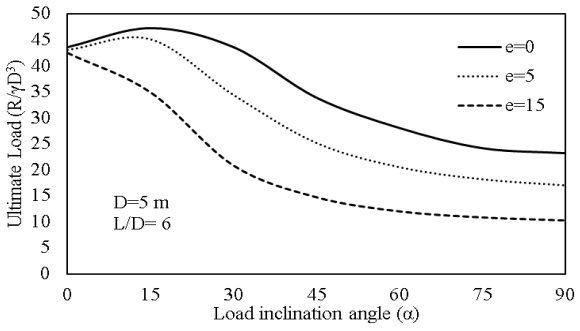

Fig. 20 The effect of the load eccentricity (e) on the ultimate load of the pile.

Conclusion

The paper presents an attempt for understanding the response of vertical piles under inclined eccentric load. The pile is embedded in loose sand. Piles with various pile lengths and pile diameters were analyzed.

The study revealed the following conclusions:

1) When the pile is pre-loaded by a vertical load the lateral load-lateral displacement relationship of the pile and consequently pile ultimate lateral load and pile lateral stiffness are not affected by the magnitude of the vertical load, while the vertical displacement of the pile due to vertical load decreases with the increase of lateral pre-load. consequently, the lateral pre-load has appreciable effect on pile vertical stiffness and pile ultimate load.
2) The load inclination angle α has appreciable effect on pile displacement U, in a way that U increase as α increased.
3) The ultimate load at polar diagrams shows that the inclination angle affects the ultimate load and the vertical component of the load R, whereas the horizontal component of any inclination angle is almost the same. Except at α equal to 15˚.
4) The pile displacement (U) has an inclination angle (β) with the vertical bigger than the load inclination angle (α). the pile displacement vector (U) is mainly due to the lateral displacement component and less contribution from vertical displacement component.
5) For α equal to and bigger than 15˚, the pile exhibits flexural behavior, and a passive wedge is developing in the soil along the top portion of the pile with shear displacement of soil oblique upward. For values of α less than 15˚, the axial behavior of the pile is prevailing, with the downward shear displacement of soil along the full length of the pile, and at the pile tip.
6) The load eccentricity (e) has an appreciable effect on the ultimate pile load in a way that the ultimate load increases as load eccentricity (e) decrease. When α is equal to zero, there is no effect of (e).

References

[1] Zhang L, Silva F and Grismala R 2005 Ultimate Lateral Resistance to Piles in Cohesionless Soils *J. Geotech. Geoenvironmental Eng.* 131 78–83

[2] Chari T R and Meyerhof G G 1983 Ultimate capacity of rigid single piles under inclined loads in sand. *Can. Geotech. J.* 20 849–54

[3] Meyerhof G G 1981 Bearing capacity of rigid piles and pile groups under inclined loads in clay. *Can. Geotech. J.* 18 297–300

[4] Sastry V V R N, Meyerhof G G and Koumoto T 1986 Behaviour of rigid piles in layered soils under eccentric and inclined loads. *Can. Geotech. J.* 23 451–7

[5] Meyerhof G G and Ranjan G 1972 The Bearing Capacity of Rigid Piles Under Inclined Loads in Sand. I: Vertical Piles *Can. Geotech. J.* 9 430–46

[6] Roy S, Chattapadhyay B C and Sahu R B 2013 Pile behavior under inclined compressive loads-A model study *Electron. J. Geotech. Eng.* 18 K 2187–205

[7] Davisson M, Proc/Canada/ K R-S M & F E C and 1965 undefined Bending and buckling of partially embedded piles *trid.trb.org*

[8] Ramasamy G 1974 *Flexural behaviour of axially and laterally loaded individual piles and group of piles* (Indian institute of Science)

[9] Goryunov B F 1973 Analysis of piles subjected to the combined action of vertical and horizontal loads (discussion) *Soil Mech. Found. Eng. 1973 101* 10 10–3

[10] Pise P J 1975 Investigations on laterally loaded pile groups *Symposium on Recent Developments in the Analysis of Soil Behavior and their Application to Geotechnical Structures, Sydney, Australia* pp 129–44

[11] Sorochan E A and Bykov V I 1976 Performance of groups of cast-in place piles subject to horizontal loading *Soil Mech. Found. Eng. 1976 133* 13 157–61

[12] Jain N K, Ranjan G and Ramasamy G 1987 Effect of vertical load on flexural behaviour of piles *Geotech. Eng.* 18

[13] Bartolomey A A 1977 Experimental analysis of pile groups under lateral loads *Proceedings of the Special Session 10 of the Ninth International Conference on Soil Mechanics and Foundation Engineering* pp 187–8

[14] Zhukov N V. and Balov I L 1978 Investigation of the effect of a vertical surcharge on horizontal displacements and resistance of pile columns to horizontal loads *Soil Mech. Found. Eng.* 15 16–22

[15] Anagnostopoulos C and Georgiadis M 1993 Interaction of Axial and Lateral Pile Responses *J. Geotech. Eng.* 119 793–8

[16] Conte E, Troncone A and Vena M 2015 Behaviour of flexible piles subjected to inclined loads *Comput. Geotech.* 69 199–209

[17] S. K, T. R V V G S and K. R 2007 Numerical Investigation of the Effect of Vertical Load on the Lateral Response of Piles *J. Geotech. Geoenvironmental Eng.* 133 512–21

[18] Hu Q, Han F, Prezzi M, Salgado R and Zhao M 2022 Finite-Element Analysis of the Lateral Load Response of Monopiles in Layered Sand *J. Geotech. Geoenvironmental Eng.* 148 04022001

[19] Abdel-Rahman K and Achmus M 2006 Numerical modelling of the combined axial and lateral loading of vertical piles *Proc. 6th Eur. Conf. Numer. Methods Geotech. Eng. - Numer. Methods Geotech. Eng.* 575–81